Faraday rotation by the undisturbed bulk and by photoinduced giant polarons in EuTe

A. B. Henriques[1] and P. A. Usachev[1,2]
[1]*Instituto de Fisica, Universidade de Sao Paulo, 05508-090 Sao Paulo, Brazil*
[2]*Ioffe Institute, 194021 St. Petersburg, Russia*

(Received 10 September 2017; revised manuscript received 6 November 2017; published 27 November 2017)

A quantum mechanical model is developed for the Faraday effect in europium telluride, for photons of energy within the transparency gap. The model is based on the well known band edge electronic energy states in EuTe. A concise expression for the Verdet constant is obtained, determined by few parameters already available in the literature. The Verdet constant adopted here, defined by the ratio between the Faraday rotation angle and the magnetization, is in effect temperature independent. Its dependence on the photon energy and applied magnetic field is in excellent agreement with published results. Below 3 T the Verdet constant is also nearly independent on field, but above 3 T at low temperatures it increases due to the band gap redshift. The model is used to calculate the photoinduced Faraday rotation associated with photoinduced giant magnetic polarons in EuTe. The theoretical photoinduced Faraday rotation excitation describes quite well the main features seen experimentally. Due to the common band-edge electronic energy structure, the model reported here could be extended to all other europium chalcogenides.

DOI: 10.1103/PhysRevB.96.195210

I. INTRODUCTION

All-optical control of the magnetic state of matter is a topic of much interest both from the fundamental point of view as well as due to device applications [1]. Recently it has been demonstrated that light can generate huge magnetic polarons in EuTe. The photoinduction of magnetic polarons was first deduced from a shift of the band-edge photoluminescence [2]. Photoluminescence is the experimental technique that has been traditionally used to investigate magnetic polaron phenomena, with the main focus on diluted magnetic semiconductors (DMS) [3]. More recently, the muon spin rotation technique has been used to investigate magnetic polarons in concentrated magnetic semiconductors [4].

However, the magnetic moment of nearly 10^3 Bohr magnetons of a photoinduced polaron in EuTe is more than an order of magnitude larger than polarons seen in DMS or detected by muon investigations, which have been estimated at a few tens of Bohr magnetons [4–6]. The giant photoinduced magnetic polarons can be easily oriented by a small magnetic field to produce a large photoinduced magnetization, which can be detected by Faraday rotation, as reported in Ref. [7]. This achievement opens up the prospect of all-optical control of magnetism in europium chalcogenides. Moreover, because of their intrinsic character, europium chalcogenides are free from alloy-related inhomogeinities that plague diluted magnetic semiconductors. It has been recently shown that EuO epitaxial layers of very high purity and crystalline quality can be grown on silicon substrates [8–10], which further increases the prospect of device applications of europium chalcogenides.

In this paper we investigate theoretically the Faraday rotation produced by an undisturbed EuTe sample, as illustrated by Fig. 1(a), and by a sample illuminated with near band gap photons—*photoinduced* Faraday rotation, as illustrated in Fig. 1(b). Despite the large amount of experimental investigations of the Faraday effect in the whole family of europium chalcogenides EuX (X = O, S, Se, Te) [11], most of the analysis has been done within a phenomenological approach [12], and a quantum mechanical theoretical model based on the known electronic energy structure specific for EuX is still lacking. In this paper such a quantum mechanical model is developed. The model is based on a well known energy level scheme and electronic quantum states that successfully described linear [13] and nonlinear [14–16] band-edge magneto-optical properties in EuX. The model describes quite well the observed Faraday rotations (for a sample in the dark and under illumination) previously reported by us and other authors, as a function of probe and pump wavelength or applied magnetic field. Our model for Faraday rotation could be applied not only to EuTe, but to the whole family of europium chalcogenides, which are described by the same band edge electronic structure. This study offers progress toward a better understanding of the interaction between polarized light and charge carriers in magnetic materials.

II. MODEL

A. Faraday rotation by the undisturbed bulk of a semiconductor: General theory

We shall describe the calculation of the Faraday rotation suffered by photons of energy in the transparency gap of an

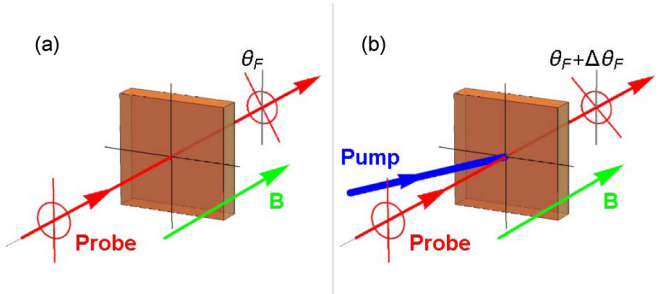

FIG. 1. Faraday rotations considered theoretically in this work. (a) Faraday rotation by the undisturbed bulk: The plane of polarization of the linearly polarized probe undergoes a rotation by an angle θ_F. (b) Photoinduced Faraday rotation: Illumination of the sample by a pump light above the band gap causes an additional rotation of the plane of polarization of the probe by $\Delta\theta_F$.

undisturbed semiconductor. As deduced by Becquerel [17], when linearly polarized monochromatic light of wavelength λ crosses a magnetized medium of thickness d, the plane of polarization undergoes a rotation by a Faraday angle given by

$$\theta_F = \frac{\pi d}{\lambda}(n_+ - n_-), \tag{1}$$

where n_+ (n_-) is the index of refraction for right- (left-) hand circularly polarized light.

Next we shall calculate the index of refraction for circularly polarized light. We consider the incidence of a circularly polarized monochromatic electromagnetic wave traveling along z and of wave vector k_z, carrying an electric field

$$\boldsymbol{E}(z,t) = \frac{\hat{x} \pm i\hat{y}}{2} E_0 e^{ik_z - i\omega t} + \text{c.c.}, \tag{2}$$

where the plus sign is associated with a right-hand circularly polarized wave (RHC), and the minus sign with a left-hand circularly polarized one (LHC) [18]. The circulating electric field of the incident wave will induce a circulating polarization vector in the material. The interaction between an electron and the electromagnetic wave can be described by the Hamiltonian [19,20]

$$\mathcal{H} = -\boldsymbol{\mu} \cdot \boldsymbol{E}(z,t), \tag{3}$$

where $\boldsymbol{\mu} = -e\sum_i \boldsymbol{r}_i$ is the electric dipole momentum operator for the electrons involved in the excitation and $-e$ is the charge of an electron. The induced circular polarization in a medium, when electrons are in a state Ψ, is given by the expectation value

$$\boldsymbol{P} = N \langle \Psi | \boldsymbol{\mu} | \Psi \rangle , \tag{4}$$

where N is the density of oscillators.

The effect of the time-dependent potential energy (3) upon the electronic wave functions can be described by standard time-dependent perturbation theory. In a typical semiconductor the band gap is of the order of 1 eV, therefore all electrons will be found in the ground state. Then in the electric dipole approximation, the lowest-order contribution to the photoinduced polarization, linear in the electric field amplitude of the incident wave, is found to be [19]

$$\boldsymbol{P}_\pm = N \sum_m \frac{\boldsymbol{\mu}_{gm}[\boldsymbol{\mu}_{mg} \cdot \boldsymbol{E}_\pm]}{E_{mg} - \hbar\omega} e^{-i\omega t} + \text{c.c.}, \tag{5}$$

where

$$\boldsymbol{E}_\pm = \frac{\hat{x} \pm i\hat{y}}{2} E_0, \tag{6}$$

and $\boldsymbol{\mu}_{mg}$ represents the electric dipole transition moment

$$\boldsymbol{\mu}_{mg} = \langle m | \boldsymbol{\mu} | g \rangle \tag{7}$$

between the ground state $|g\rangle$ and an excited state $|m\rangle$. In Eq. (5) the plus sign gives the polarization induced by RHC, and the minus for LHC. $E_{mg} = E_m - E_g$ is the energy gap between the ground state and the m state. In deducing $\boldsymbol{P}_\pm$ given in (5), antiresonant terms, associated with $(E_{mg} + \hbar\omega)$ in the denominator, have been discarded, because all m states are of energy approximating the band gap, and we are considering Faraday rotation of photons below the gap, but in close resonance to it.

For an isotropic medium symmetry considerations impose that the induced polarization be parallel to the external electric field [19]

$$\boldsymbol{P}_\pm = \varepsilon_0 \chi_\pm \boldsymbol{E}_\pm e^{-i\omega t} + \text{c.c.} \tag{8}$$

where $\varepsilon_0 = 8.85 \times 10^{-12}\ \text{C}^2/\text{J m}$, and $\chi_\pm$ is the linear electrical susceptibility for RHC (plus sign) or LHC (minus sign). To obtain the susceptibility in the isotropic approximation, we project vector $\boldsymbol{\mu}_{gm}$ onto the electric field vector of the circularly polarized electromagnetic wave. This procedure leads to

$$\chi_\pm = \frac{N}{2\varepsilon_0} \sum_m \frac{|\mu^\pm_{mg}|^2}{E_{mg} - \hbar\omega}, \tag{9}$$

where $\mu^\pm_{mg}$ represents the electric dipole transition moment for circularly polarized light

$$\mu^\pm_{mg} = -e \langle m | x_i \pm i y_i | g \rangle , \tag{10}$$

with x_i, y_i being the Cartesian coordinates of the electrons involved.

The index of refraction for circularly polarized light can be obtained from (9):

$$n_\pm = \sqrt{1 + \chi_\pm}. \tag{11}$$

Therefore

$$n_+ - n_- = \frac{n_+^2 - n_-^2}{n_+ + n_-} = \frac{1}{2n}(\chi_+ - \chi_-), \tag{12}$$

where $n = \frac{n_+ + n_-}{2}$. Using (1) and (9) we finally get

$$\theta_F = \frac{\pi d}{\lambda} \frac{N}{4\varepsilon_0 n} \sum_m \frac{D_{mg}}{E_{mg} - \hbar\omega}, \tag{13}$$

where

$$D_{mg} = |\mu^+_{mg}|^2 - |\mu^-_{mg}|^2. \tag{14}$$

Formula (13) together with (14) is applicable to any magnetic semiconductor with a gap between the ground state and a set of excited states closely spaced in energy at the band edge.

B. Band-edge energy level scheme for EuTe

The energy level scheme used in our model for the Faraday effect in EuTe is shown in Fig. 2. The ground state of an Eu atom is described by the term symbol $^8S_{7/2}$, which is built from seven electrons in a $4f$ orbital. The $^8S_{7/2}$ electrons are strongly localized around an Eu atom, they are shielded from the environment by more extended $5p$ electrons, and therefore can be described by the $4f$ wave functions of an isolated Eu atom. We shall represent the ground state of the seven electrons by the ket vector:

$$|^8S_{7/2}\rangle . \tag{15}$$

The lowest-energy excited electronic states of EuTe require describing simultaneously seven electrons, as follows. One of the seven electrons comprising the $^8S_{7/2}$ term is transferred to the conduction band built from Eu d orbitals. The six remaining valence electrons generate a manifold of seven energy levels due to the spin-orbit splitting, and are described by the term symbol $^7F_{JM}$ ($J = 0, \ldots, 6$ is the total angular

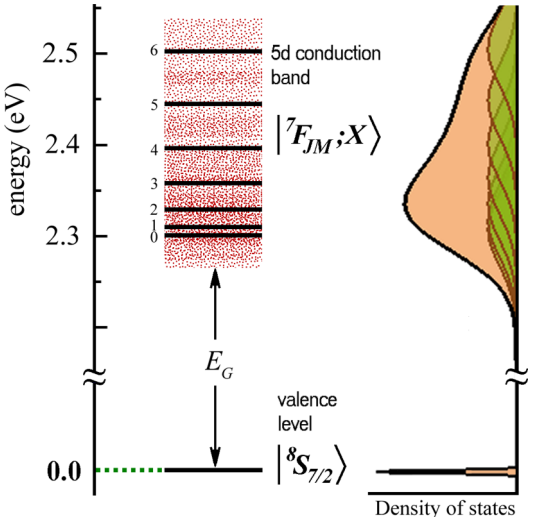

FIG. 2. Ground state $|^8S_{7/2}\rangle$ and lowest-energy excited states $|^7F_{JM};X\rangle$ in EuTe. Black horizontal lines indicate the positions of the $J = 0,\ldots,6$ Landé ladder associated with the spin-orbit splitting of the term $^7F_{JM}$ (with a spin-orbit constant of $\lambda_{4f} = 9.6$ meV). Each Landé level is broadened by the energy width of the $5d(t_{2g})$ conduction band, taken to be 80 meV.

momentum quantum number, and M is the projection quantum number for the total angular momentum). The energy of this excitation depends on the exact state in which the six electrons comprising the $^7F_{JM}$ term are left.

Thus, the lowest energy electronic excitations of an EuTe crystal are associated with six electrons forming the term $^7F_{JM}$ and an electron in a narrow d-conduction band. The wave function of such an excited state is described by the quantum numbers J and M, plus a set of quantum numbers X, associated with the electron in the d-conduction band. Such an excited state can be represented by the ket

$$|JMX\rangle = |^7F_{JM};\,X\rangle\,. \tag{16}$$

In a calculation of the Faraday rotation for photons below the bandgap, the small energy dispersion of the d-conduction band may be ignored, hence the energy gap between the excited states and the ground state will be independent of X and determined solely by J:

$$E_J = E_G + \tfrac{1}{2}\lambda_{4f}J(J+1), \tag{17}$$

where λ_{4f} is the spin-orbit constant for the $^7F_{JM}$ term, and E_G is the EuTe band gap. The Zeeman energy has been disregarded because of its small magnitude [14].

C. Choice of a Verdet constant for EuTe

The Verdet constant V of materials of zero spontaneous magnetization is commonly defined by the relation [11,20–23]

$$\theta_F = V\,B\,d, \tag{18}$$

where d is the thickness of the magnetized region and B is the magnetic field. However, the real source of the Faraday rotation is the magnetization of the material and not the magnetic field by itself, which causes the Verdet constant so defined to be temperature dependent. For example, in EuTe, the magnetization M at a given magnetic field varies hugely with temperature, hence the Verdet constant defined by (18) shows a dramatic temperature dependence of several orders of magnitude in a ten degree interval, as shown in Ref. [23].

An alternative definition of the Verdet constant, sometimes addressed as Kundt constant [22,24], and used to describe Faraday rotation by ferromagnetic materials, is given by the formula

$$\theta_F = V\,M\,d. \tag{19}$$

Although EuTe is an antiferromagnet, thus it has no spontaneous magnetization, its Faraday rotation can also be described by (19), as shown in Ref. [25]. The definition of the Verdet constant through (19) connects the Faraday rotation directly to the magnetization, which corresponds to a specific electronic state of the material. Therefore such a Verdet constant measures the optical rotation power, or circular susceptibility, associated with a specific electronic state of the material under study. The rotation power will be temperature independent as long as the material's electronic band-edge energy spectrum and its occupation remains unaffected by temperature. The pure connection to the electronic structure and its independence on temperature make the Verdet constant defined by (19) very attractive. It is also very practical, for instance, it can be used to determine the demagnetizating field at any temperature and applied magnetic field [25]. Therefore we shall henceforward adopt the Verdet constant defined by (19).

D. Faraday rotation by the undisturbed EuTe bulk

In order to apply the results of Sec. II A to EuTe, we make the following substitutions in Eqs. (13) and (14):

(1) $|g\rangle = |^8S_{7/2}\rangle$—see (15);
(2) $|m\rangle = |JMX\rangle$—see (16);
(3) $E_{mg} = E_J$—see (17);
(4) $N = 4/a^3$ is the density of Eu atoms in the face centered cubic lattice of parameter $a = 6.6$ Å [26];
(5) we also assume that the optical absorption in EuTe is isotropic, based on direct experimental results (see Fig. 1 in Ref. [13]).

These substitutions lead to

$$\theta_F = \frac{\pi d}{\lambda}\frac{N}{4\varepsilon_0 n}\sum_{JMX}\frac{D_{JMX}}{E_J - \hbar\omega}, \tag{20}$$

where

$$D_{JMX} = |\mu^+(JMX)|^2 - |\mu^-(JMX)|^2 \tag{21}$$

and

$$\mu^{\pm}(JMX) = -e\langle^8S_{7/2}|\sum_{i=1}^{7}(x_i \pm iy_i)|^7F_{JM};X\rangle. \tag{22}$$

In Eq. (22) x_i, y_i are electron Cartesian coordinates in the reference frame in which z points along the photon wave vector, whereas the wave function for $|^8S_{7/2}\rangle$ and $|^7F_{JM}\rangle$ states have electron angular momenta defined in the reference frame of the lattice spins. At $T = 0$ K and for an applied magnetic field B smaller than the saturation field $B_{\rm SAT}$, the lattice spins are divided into two sublattices, in which the Eu spins are

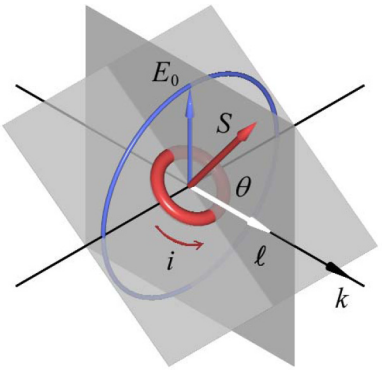

FIG. 3. Monochromatic circularly polarized light with wave vector $\boldsymbol{k}$, described by a rotating electric field of modulus E_0, and carrying an angular momentum $\boldsymbol{\ell}$ is incident on a current loop i, associated with spin $\boldsymbol{S}$. The angle between $\boldsymbol{\ell}$ and $\boldsymbol{S}$ is θ. Because the current loop is rigidly defined by strong atomic forces, only the $\boldsymbol{\ell}$ component parallel to $\boldsymbol{S}$ can perturb the current.

oriented at an angle 2θ to each other and an angle θ to the magnetic field, such that [27–30]

$$\cos\theta = \frac{B}{B_{\mathrm{SAT}}}. \tag{23}$$

In the Faraday geometry considered in this work θ is precisely the angle between the light wave vector k_z and the sublattice spins. A calculation of the matrix element $\mu^{\pm}(JMX)$ using (22) requires formulating the wave functions in the photon reference frame, which can be done by Euler rotations, using Wigner matrices [31]. The calculation of matrix elements involving $|^8S_{7/2}\rangle$ and $|^7F_{JM};X\rangle$ states, using Wigner matrices, is described in detail in Refs. [13,14,32], and the result is expressed in terms of a constant r_{df}, i.e., the $4f$-$5d$ radial integral.

However, for the purposes of this work, there is a simpler alternative, which circumvents the complicated Wigner rotations, and which is based on the following argument from semiclassical mechanics, illustrated in Fig. 3. A semiclassical spin vector $\boldsymbol{S}$ represents a circular current loop in a plane perpendicular to $\boldsymbol{S}$. Circularly polarized light traveling along z carries a rotating electric field vector and an angular momentum that can be transferred to the charges in the loop and will increment the spin, and this increment corresponds to a photoinduced circular polarization. However, because the circulating charges are confined to a loop that is rigidly determined by strong interatomic forces, the only effect light may cause is a perturbative increase in the current, meaning that only the light angular momentum component parallel to $\boldsymbol{S}$ can photoinduce polarization. Therefore, when the angle between $\boldsymbol{S}$ and the z axis is increased from zero to θ, the photoinduced polarization will be reduced by a factor of $\cos\theta$. Therefore, using (23), we can rewrite (20) as

$$\theta_F = \frac{B}{B_{\mathrm{SAT}}}\frac{\pi d}{\lambda}\frac{N}{4\varepsilon_0 n}\sum_{JMX}\frac{D^{\parallel}_{JMX}}{E_J-\hbar\omega}, \tag{24}$$

where

$$D^{\parallel}_{JMX} = |\mu^{+}_{\parallel}(JMX)|^2 - |\mu^{-}_{\parallel}(JMX)|^2 \tag{25}$$

and

$$\mu^{\pm}_{\parallel}(JMX) = -e\langle {}^8S_{7/2}|\sum_{i=1}^{7}(x_i \pm iy_i)|{}^7F_{JM};X\rangle_{\parallel}. \tag{26}$$

The index $\parallel$ indicates that the matrix element is to be calculated when all lattice spins point in the z direction (the direction of the photon wave vector), which circumvents Wigner rotations for the calculation of the electric dipole matrix elements.

It should be noticed that the semiclassical argument does not involve any new approximations, it only requires that the incident light is a small perturbation on the system producing the Faraday rotation, but this assumption was already made in the quantum mechanical calculation. In this case, the semiclassical and quantum mechanical calculations are expected to produce exactly the same result, as well as to have the same validity range. The difference between the two calculations is purely mathematical. One is a complex calculation involving a very large number of matrix operations, the other substitutes all those operations by a simple multiplication by a cosine. Of course, it would be a huge task to demonstrate formally that the enormous formula produced by the quantum mechanical calculation can be simplified into a multiplication by a cosine. In this work we limited ourselves to comparing the numerical output of the quantum mechanical calculation given by (20), to the numerical output of the semiclassical calculation, given by (24), for a wide range of parameter. The numerical equivalence of the two calculations was confirmed, which is sufficient for the purposes of this work,

A further advantage of the semiclassical result is that formula (24) allows us to express the Faraday rotation angle as directly proportional to the magnetization, and hence allowing us to extract an explicit expression for the Verdet constant in the quantum mechanical picture. Indeed, (23) implies that at low temperatures, the magnetization is linearly dependent on the applied magnetic field

$$M = \frac{B}{B_{\mathrm{SAT}}}M_{\mathrm{SAT}}, \tag{27}$$

where $M_{\mathrm{SAT}} = N\mu_{\mathrm{Eu}}$, $\mu_{\mathrm{Eu}} = g\mu_B S$ is the magnetic moment of an Eu atom, $g = 2$ is the gyromagnetic factor for an Eu atom in the $^8S_{7/2}$, μ_B is the Bohr magneton, $S = 7/2$ is the spin of an Eu atom, and $B_{\mathrm{SAT}} = 8.3$ T is the magnetic field required to saturate the magnetization in the Faraday geometry [28]. This result is confirmed by direct magnetization measurements [29]. Substituting (27) in (24) and using (19) we get

$$V = \frac{\pi}{\lambda}\frac{N}{4\varepsilon_0 n\, M_{\mathrm{SAT}}}\sum_{JMX}\frac{D^{\parallel}_{JMX}}{E_J-\hbar\omega}. \tag{28}$$

In contrast to (24), which is valid only for $T = 0$ K, for EuTe (19) will be also valid for $T > 0$ K if (28) is used, because the temperature dependence is coded in the magnetization M. The temperature validity range of (19) and (28) is discussed further in the next section.

III. RESULT OF THE CALCULATIONS

A. Faraday rotation by the undisturbed EuTe bulk

The Verdet constant for EuTe was calculated as a function of photon energy using (28). The parameters used in the

TABLE I. EuTe parameters, used in the Verdet constant calculation.

Parameter	E_G (eV)	a (Å)	r_{df} (Å)	λ_{4f} (meV)
Value	2.3	6.6	0.2	9.6
References	[28,33]	[11]	[34]	[34]

calculations are shown in Table I. Figure 4 represents the theoretical result by the full line. The dots shown in Fig. 4 depict experimental results from the literature. There is very good agreement between theory and experiment, in a wide range of photon energies, demonstrating the reliability of the model. The fast growth of the Verdet constant when the photon energy approaches the EuTe band gap is well described by theory. The reason behind this increase is the increasing photoinduced polarization when the incident photons approach resonance with the band gap. This is reflected by Eq. (28), in which the difference between the band gap and photon energies appears in the denominator.

As an additional test of the theory we next consider the magnetic field dependence of the Verdet constant. It is well known that in EuTe the Faraday rotation at a given photon energy increases superlinearly when the applied magnetic field exceeds 2–3 T [34–36]. The reason behind the fast increase of the Verdet constant is the redshift of the EuTe band gap, which below the Néel temperature varies quadratically with the magnetic field until saturation [2]

$$E_G(B) = E_G(0) - J_{df} S \begin{cases} \left(\frac{B}{B_{\rm SAT}}\right)^2 & \text{if } B \leqslant B_{\rm SAT}, \\ 1 & \text{if } B > B_{\rm SAT}. \end{cases} \quad (29)$$

This formula reflects the fact that the Zeeman interaction favors alignment of lattice spins with the applied magnetic field, which in turn reduces the exchange energy of a band-edge electron. For fields greater than $B_{\rm SAT}$ the lattice spins attain ferromagnetic alignment, and the gap becomes constant. The faster than linear growth of the Verdet constant when a magnetic field is applied is perfectly described by (28), if

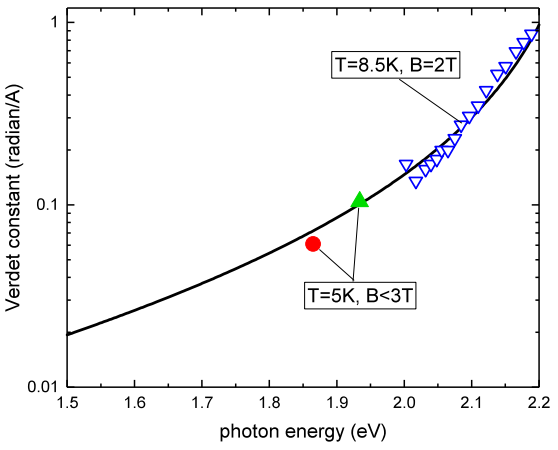

FIG. 4. Calculated Verdet constant as a function of photon energy for low magnetic fields. The circle and the full triangle are experimental results for 1.865 and 1.934 eV, from Refs. [25,34], respectively. The inverted empty triangles were taken from Ref. [35].

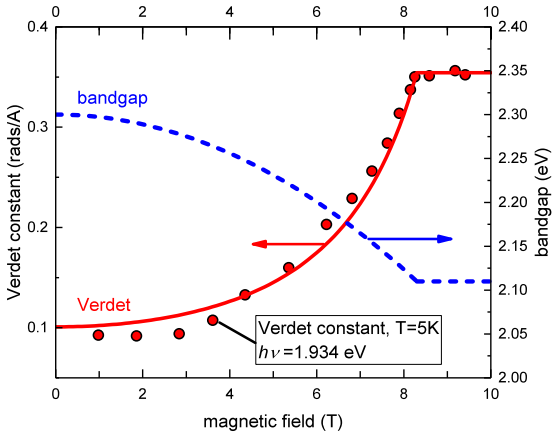

FIG. 5. Calculated Verdet constant as a function of magnetic field for a photon energy of $\hbar\omega = 1.934$ eV (full line). The circles represent experimental results for $T = 5$ K (taken from Ref. [34]). The parameters used in the calculation where taken from Table I, and additionally the band gap redshift was calculated as described in Ref. [13] using an exchange constant $J_{df} S = 190$ meV. The ban gap dependence, given by (29), is shown by the dashed curve.

the shrinking band gap given by (29) is substituted into (17), which defines E_J. Notice that $E_J - \hbar\omega$ enters the denominator appearing in (28), hence when the band gap shrinks, the photon energy becomes more resonant with the band gap, the denominator in (28) decreases. Therefore in a magnetic field the Verdet constant increases faster and faster until saturation at $B = B_{\rm SAT}$, and then becomes constant when the band gap stops shrinking. The result of the calculation is presented in Fig. 5, showing excellent agreement with the experiment. Also shown in Fig. 5 is the band gap dependence on B as given by Eq. (29), to demonstrate that a change in the Verdet constant correlates with a band gap shift. It is to be observed that the Verdet constant is almost independent on field in the 0–3 T interval, because in this range of fields a redshift of the optical absorption band gap is almost absent [2,34].

Formula (28) shows that the Verdet constant is determined solely by the band-edge electronic structure: the width of the band gap, the energy position of the conduction band energy levels and their respective wave functions. In intrinsic EuTe, whose band gap is over 2 eV, these levels will not be populated up to well above room temperature. The only way temperature may affect the Verdet constant is through a shift of the energy levels, as for example detected by Wachter in EuSe in the temperature range 2–30 K [27]. Thus, a temperature dependence of the Verdet constant is associated with the temperature dependence of the band gap. Analogously, the magnetic field dependence of the Verdet constant is also associated with changes in the band gap (caused by the magnetic field in this case), as demonstrated above (see Fig. 5). Because the band gap shows little temperature dependence in low magnetic fields, the assumption of a temperature-independent Verdet constant made in Ref. [25] is solidly justified.

It should be stressed that the effectively temperature independent Verdet constant obtained in this work, and given by (28), is defined by the ratio of the Faraday rotation angle to the magnetization. Notice that the Faraday rotation angle is hugely dependent on temperature, however, the use of our Verdet

constant definition transfers all this huge temperature dependence to the magnetization, and not to the Verdet constant. This is in sharp contrast to the commonly used Verdet constant for antiferromagnets and paramagnets, defined by the ratio of the Faraday rotation angle to the magnetic field, in which case the Verdet constant becomes hugely dependent on temperature. For instance, the usual Verdet constant for EuTe was measured in Ref. [23], and it changes by several orders of magnitude in a narrow temperature range around the critical temperature of about 10 K. The enormous temperature dependence of the Verdet constant seen in Ref. [23] simply reflects the temperature dependence of the magnetization. From this point of view, the definition of a Verdet constant used in this work is highly advantageous, because it is essentially temperature independent. Its temperature dependence is tied to the variation of the band gap and of the band-edge energy levels, therefore we expect only a very small variation in the 0–300 K temperature range. The temperature dependence of our Verdet constant is analogous to that of the refraction index, which is also tied to variations of the band gap [37], and shows variations by at most a few percent in the 0–300 K temperature range [38].

B. Photoinduced Faraday rotation in EuTe

In the previous section we discussed the Faraday rotation of photons with energy less than the band gap when the EuTe sample is undisturbed (in the dark). However, if the sample is illuminated with light of energy larger than the band gap, electrons are photoexcited into the conduction band, which can cause an additional Faraday rotation, as illustrated in Fig. 1(b), which is the subject of the present subsection. In a magnetic semiconductor such as EuTe, electrons in the conduction band interact strongly with the lattice spins through the *d-f* exchange interaction. The *d-f* exchange interaction favors the alignment of the lattice spins, forming a spherical magnetic polaron [3,39], sometimes also named *spin polaron* [40]. The size of the magnetic polaron in EuTe at low temperatures is $\mu_{\mathrm{Pol}} = 610\,\mu_B$ [41]. Because of the large magnetic moment of an individual polaron, an ensemble of photoexcited polarons displays superparamagnetic behavior [7,42], and the application of only a small magnetic field is sufficient to align all polarons into a common direction, producing a photoinduced polaron magnetization equal to $n_{\mathrm{Pol}}\mu_{\mathrm{Pol}}$, where n_{Pol} is the steady-state density of photoinduced polarons. Due to their large radius [41], photoinduced polarons have a large effective mass, which makes them immobile [25,40]. Moreover, the $4f$ hole that stabilizes the polaron [41] is very heavy, and anchors the polaron. Therefore, photoinduced polarons do not drift away from the position where they were generated, meaning that photoexcited polarons are confined in a layer of thickness equal to the penetration depth of the excitation light. The penetration depth of the pump light, of energy $\hbar\omega$, is of the order of $1/\alpha(\hbar\omega)$, where α is the absorption coefficient. We can therefore estimate the maximum photoinduced Faraday rotation angle from (19), if we substitute M by $n_{\mathrm{Pol}}\mu_{\mathrm{Pol}}$ and d by $1/\alpha(\hbar\omega)$:

$$\Delta\theta_F = V\, n_{\mathrm{Pol}}\mu_{\mathrm{Pol}}\,\frac{1}{\alpha(\hbar\omega)}. \tag{30}$$

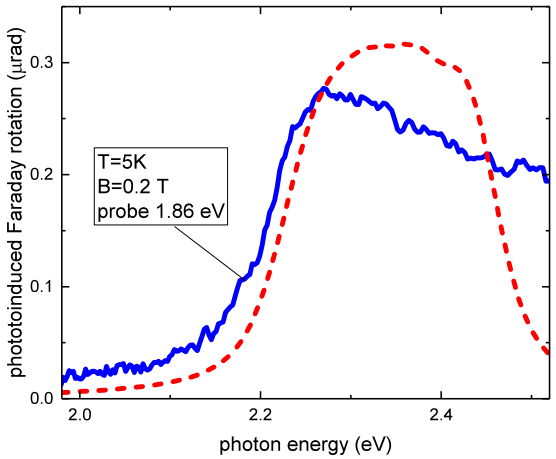

FIG. 6. Photoinduced Faraday rotation. The full line shows the experimental result, taken from Ref. [7]. The pump intensity was $p = 20\ \mathrm{mW/cm^2}$ and the probe photons had energy 1.86 eV.

The steady-state population of polarons is approximately given by [25]

$$n_{\mathrm{Pol}} = \chi(\hbar\omega)\frac{p\alpha(\hbar\omega)\tau_0}{\hbar\omega}, \tag{31}$$

where $\chi(\hbar\omega)$ is the quantum efficiency (the number of photogenerated polarons per incident pump photon), p is the intensity of the pump light, and τ_0 is the magnetic polaron lifetime. Substitution of (31) in (30) gives

$$\Delta\theta_F = V\,\chi(\hbar\omega)\,\frac{p\mu_{\mathrm{Pol}}\tau_0}{\hbar\omega}. \tag{32}$$

The quantum efficiency depends on the pump energy through the absorption coefficient, so we can write

$$\chi(\hbar\omega) = \frac{\alpha(\hbar\omega)}{\alpha(\hbar\omega_0)}\chi(\hbar\omega_0), \tag{33}$$

where $\hbar\omega_0$ is a certain pump energy for which the quantum efficiency is known. Thus we arrive at the final expression for the photoinduced Faraday rotation angle

$$\Delta\theta_F = V\,\frac{\alpha(\hbar\omega)}{\alpha(\hbar\omega_0)}\chi(\hbar\omega_0)\,\frac{p\mu_{\mathrm{Pol}}\tau_0}{\hbar\omega}. \tag{34}$$

Figure 6 shows by the full line the experimental photoinduced Faraday rotation excitation spectrum (from Ref. [7]), taken at $T = 5$ K and a magnetic field of 200 mT, which is sufficient to align all polarons. The dashed line shows the theoretical result, produced by (34). The absorption coefficient $\alpha(\hbar\omega)$ entering (34) was calculated as described in Ref. [13]. The parameters used in the calculation were taken from Tables I and II. The theory gives an approximate description

TABLE II. EuTe parameters used in the photoinduced Faraday rotation calculation. Δ_d is the full width at half maximum of the d-conduction band.

Parameter	Δ_d (meV)	μ_{Pol} (μ_B)	τ_0 (μs)	χ ($\hbar\omega_0 = 2.33$ eV)
Value	80	610	15	0.1
References	[13,14]	[2,7,41]	[7]	[25]

of the experimental observations: (1) a sharp rise of the photoinduced Faraday rotation when the excitation photons reach resonance with the band gap. (2) The size of the step of the calculated photoinduced Faraday angle at the resonance (0.32 μrad) agrees with the measured value (0.27 μrad) within the experimental error, estimated around 10%–15%. The theory also predicts a reduction of the photoinduced effect above the resonance, seen in the experiment. On the other hand, our theory can only account for the photoinduced Faraday rotation at most about ∼200 meV above the band gap, which is the width of the conduction band associated with $|^7F_{JM};\ X\rangle$ states (see Fig. 2). Therefore for larger excitation energies the theory produces zero photoinduced Faraday rotation, whereas experimentally the photoinduced Faraday rotation persists, due to electronic excitations into the background states not included in our model.

IV. CONCLUSIONS

In conclusion, we have developed a quantum mechanical model for below-the-gap Faraday rotation in EuTe, on the basis of a band edge electronic energy structure that is well established. The model is dependent on very few parameters, which are well known from the literature. The validity of the model is demonstrated by its comparison to a wide range of experimental data. An important result of the model is the obtention of a nearly temperature independent Verdet constant. To the best of our knowledge, this is the first report of a quantum mechanical calculation of the Verdet constant defined by the ratio between the Faraday rotation and the magnetization in an antiferromagnetic material. Although the validity of the model was demonstrated for EuTe, it should remain valid for all the family of europium chalcogenides, which share the same band-edge electronic structure, and should be easily adapted to any other magnetic semiconductor.

ACKNOWLEDGMENTS

This work was supported by the Brazilian agencies CNPq (Projects 307400/2014-0 and 456188/2014-2) and FAPESP (Project 2016/24125-5), and the Russian Science Foundation (Project 17-12-01314).

[1] C.-H. Lambert, S. Mangin, B. S. D. C. S. Varaprasad, Y. K. Takahashi, M. Hehn, M. Cinchetti, G. Malinowski, K. Hono, Y. Fainman, M. Aeschlimann *et al.*, Science **345**, 1337 (2014).
[2] A. B. Henriques, G. D. Galgano, E. Abramof, B. Diaz, and P. H. O. Rappl, Appl. Phys. Lett. **99**, 091906 (2011).
[3] S. Takeyama, *Magneto-optics*, Vol. 128 of Springer Series in Solid State Science (Springer, Berlin, 2000), pp. 179–209.
[4] V. G. Storchak, O. E. Parfenov, J. H. Brewer, P. L. Russo, S. L. Stubbs, R. L. Lichti, D. G. Eshchenko, E. Morenzoni, T. G. Aminov, V. P. Zlomanov, A. A. Vinokurov *et al.*, Phys. Rev. B **80**, 235203 (2009).
[5] P. A. Wolff, *Theory of Bound Magnetic Polarons in Semimagnetic Semiconductors*, Vol. 25 of Semiconductors and Semimetals (Academic, San Diego, 1988), p. 414.
[6] M. Nawrocki, R. Planel, G. Fishman, and R. Galazka, Phys. Rev. Lett. **46**, 735 (1981).
[7] A. B. Henriques, G. D. Galgano, P. H. O. Rappl, and E. Abramof, Phys. Rev. B **93**, 201201 (2016).
[8] A. Schmel, V. Vaithyanathan, A. Herrnberger, S. Thiel, C. Richter, M. Liberati, T. Heeg, M. Rockerath, L. F. Kourkoutis, S. Muhlbauer *et al.*, Nat. Mater. **6**, 882 (2007).
[9] D. V. Averyanov, Y. G. Sadofyev, A. M. Tokmachev, A. E. Primenko, I. A. Likhachev, and V. G. Storchak, ACS Appl. Mater. Interf. **7**, 6146 (2015).
[10] D. V. Averyanov, C. G. Karateeva, I. A. Karateev, A. M. Tokmachev, A. L. Vasiliev, S. I. Zolotarev, I. A. Likhachev, and V. G. Storchak, Sci. Rep. **6**, 22841 (2016).
[11] A. Mauger and C. Godart, Phys. Rep. **141**, 51 (1986).
[12] W. Reim and J. Schoenes, *Ferromagnetic Materials* (North-Holland, 1990), Vol. 5, Chap. 2, p. 133.
[13] A. B. Henriques, M. A. Manfrini, P. H. O. Rappl, and E. Abramof, Phys. Rev. B **77**, 035204 (2008).
[14] A. B. Henriques, E. Abramof, and P. H. O. Rappl, Phys. Rev. B **80**, 245206 (2009).
[15] B. Kaminski, M. Lafrentz, R. V. Pisarev, D. R. Yakovlev, V. V. Pavlov, V. A. Lukoshkin, A. B. Henriques, G. Springholz, G. Bauer, E. Abramof *et al.*, Phys. Rev. Lett. **103**, 057203 (2009).
[16] M. Lafrentz, D. Brunne, B. Kaminski, V. V. Pavlov, A. B. Henriques, R. V. Pisarev, D. R. Yakovlev, G. Springholz, G. Bauer, E. Abramof *et al.*, Phys. Rev. B **82**, 235206 (2010).
[17] H. Becquerel, C. R. Heb. Acad. Sci. Paris **125**, 679 (1987).
[18] R. P. Feynman, R. B. Leighton, and M. L. Sands, *The Feynman Lectures on Physics* (Addison-Wesley, Reading, MA, 1963–1965), Vol. 3, p. 11-11.
[19] R. W. Boyd, *Nonlinear Optics* (Academic, New York, 2003).
[20] P. R. Berman, Am. J. Phys. **78**, 270 (2010).
[21] Y. Xu and M. Duan, Phys. Rev. B **46**, 11636 (1992).
[22] D. Jiles, *Introduction to Magnetism and Magnetic Materials* (Chapman and Hall, Englewood Cliffs, NJ, 1998), p. 57.
[23] H. Krenn, W. Herbst, H. Pascher, Y. Ueta, G. Springholz, and G. Bauer, Phys. Rev. B **60**, 8117 (1999).
[24] E. P. Lewis, *The Effect of a Magnetic Field on Radiation* (American Book Company, Woodstock, GA, 1900), p. xi.
[25] A. B. Henriques, A. R. Naupa, P. A. Usachev, V. V. Pavlov, P. H. O. Rappl, and E. Abramof, Phys. Rev. B **95**, 045205 (2017).
[26] U. Köbler and C. Sauer, *Landolt-Bornstein - Group III Condensed Matter* (Springer, Berlin, 1982), Vol. 12C, Chap. 6.2.1, p. 167.
[27] P. Wachter, CRC Crit. Rev. Solid State Sci. **3**, 189 (1972).
[28] L. K. Hanamoto, A. B. Henriques, N. F. Oliveira, P. Rappl, E. Abramof, and Y. Ueta, J. Phys.: Condens. Matter **16**, 5597 (2004).
[29] A. B. Henriques, L. K. Hanamoto, E. T. Haar, E. Abramof, A. Y. Ueta, and P. H. O. Rappl, Int. J. Mod. Phys. B **18**, 3813 (2004).
[30] J. Feinleib and C. R. Pidgeon, Phys. Rev. Lett. **23**, 1391 (1969).
[31] L. D. Landau and E. M. Lifshitz, *Quantum Mechanics - Nonrelativistic Theory* (Pergamon, New York, 1991).
[32] A. B. Henriques, G. D. Galgano, and E. Abramof, J. Phys.: Condens. Matter **20**, 255209 (2008).
[33] W. Heiss, R. Kirchschlager, G. Springholz, Z. Chen, M. Debnath, and Y. Oka, Phys. Rev. B **70**, 035209 (2004).

[34] A. B. Henriques, A. Wierts, M. A. Manfrini, G. Springholz, P. H. O. Rappl, E. Abramof, and A. Y. Ueta, Phys. Rev. B **72**, 155337 (2005).
[35] J. Schoenes and P. Wachter, Physica B+C **86**, 125 (1977).
[36] H. Hori, R. Akimoto, M. Kobayashi, S. Miyamoto, M. Furusawa, N. M. Kreines, A. Yamagishi, and M. Date, Physica B **201**, 438 (1994).
[37] P. J. L. Hervé and L. K. J. Vandamme, J. Appl. Phys. **77**, 5476 (1977).
[38] J. Talghader and J. S. Smith, Appl. Phys. Lett. **66**, 335 (1995).
[39] D. Emin, *Polarons* (Cambridge University Press, New York, 2013), p. 65.
[40] N. F. Mott, *Metal-Insulator Transitions*, 2nd ed. (Taylor & Francis, London, 1990), Vol. 93, p. 93.
[41] A. B. Henriques, F. C. D. Moraes, G. D. Galgano, A. J. Meaney, P. C. M. Christianen, J. C. Maan, E. Abramof, and P. H. O. Rappl, Phys. Rev. B **90**, 165202 (2014).
[42] C. P. Bean and J. D. Livingston, J. Appl. Phys. **30**, 120S (1959).